

SUPPLEMENTARY INFORMATION

A benzimidazolium-based organic cage with antimicrobial activity

Sonia La Cognata¹, Donatella Armentano², Nicoletta Marchesi³, Pietro Grisoli³, Alessia Pascale³, Marion Kieffer⁴, Angelo Taglietti¹, Anthony P. Davis⁴, and Valeria Amendola^{1*}

¹ *Department of Chemistry, University of Pavia, viale T. Taramelli 12, Pavia, 27100, Italy.*

² *Department of Chemistry & Chemical Technologies, University of Calabria, Via P. Bucci, 14/C, 87036 Rende (CS) - Italy.*

³ *Department of Drug Sciences, section of Pharmacology, University of Pavia, viale T. Taramelli 12, Pavia, 27100, Italy.*

⁴ *School of Chemistry, University of Bristol, Bristol BS8 1TS, UK.*

* Correspondence: valeria.amendola@unipv.it

Index

1. Details on materials and methods	pag. S3
2. Preparation of $\mathbf{1}(\text{NO}_3)_3$	pag. S6
3. Characterization of $\mathbf{1}(\text{NO}_3)_3$	pag. S7
4. Single crystals X-ray diffraction analysis	pag. S9
5. ^1H -NMR investigations	pag. S12
6. Anion transport study on $\mathbf{1}(\text{NO}_3)_3$	pag. S17
References	pag. S18

1. Details on materials and methods

All reagents for syntheses were purchased from Sigma Aldrich or VWR and used without further purification. The synthesis of the receptor $1(\text{PF}_6)_3$ has already been reported by our group in a previous work [1]. High-resolution mass spectra were recorded on a Sciex X500B QTOF System (Framingham, U.S.A.) operated in the ESI mode. ^1H -, ^{13}C -NMR and NOESY spectra were recorded on a Bruker AVANCEIII 400 MHz, equipped with a 5 mm BBO probe head with Z-gradient (Bruker BioSpin) or Bruker AMX 300 MHz. Deuterated solvents (D_2O , CD_3CN) were purchased by Sigma Aldrich or VWR and used as received. Chemical shifts are reported in ppm with the residual solvent as the internal reference, whereas two-dimensional spectra were graphically referenced. All NMR spectra were carried out at $25.0\text{ }^\circ\text{C}$. UV-vis spectra were collected using a Varian Cary 50 SCAN spectrophotometer, using a quartz cuvette (path length = 0.1 cm), at $25.0 \pm 0.1\text{ }^\circ\text{C}$.

1.1 UV-vis. titration studies

10 mL of a solution of $1(\text{PF}_6)_3$ ($1.74 \times 10^{-4}\text{ M}$) in acetonitrile were titrated with a 100-fold more concentrated acetonitrile solution of $[\text{TBA}]\text{NO}_3$ in the same solvent ($T = 25^\circ\text{C}$). After each addition of the titrant solution, the UV-vis. spectrum was recorded (path length = 0.1 cm). Titration data were processed with the Hyperquad package [2] to determine the equilibrium constants.

1.2 ^1H -NMR titration studies

0.75 mL of a solution of $1(\text{NO}_3)_3$ (3.58 mM) in $\text{CD}_3\text{CN}/\text{D}_2\text{O}$ 4:1 (*v:v*) mixture were titrated with a 0.341 M solution of $[\text{TBA}]\text{NO}_3$ in the same solvent mixture ($T = 25^\circ\text{C}$). The titration was directly performed in the NMR tube, and after each addition of the titrant solution, the ^1H -NMR spectrum was recorded. Titration data were processed with the HypNMR program (Hyperquad package) [2] to determine the equilibrium constants.

1.3 Cytotoxicity studies

1.3.1 Cell culture

Human neuroblastoma SH-SY5Y cells were purchased from ATCC (Manassas, VA) and cultured at 37°C in T75 flasks in a humidified incubator with 5% CO_2 . SH-SY5Y cells were grown in Eagle's minimum essential medium (EMEM) supplemented with 10% fetal bovine serum, 1% penicillin–streptomycin, L-glutamine (2 mM), non-essential amino acids (1 mM), and sodium pyruvate (1 mM).

1.3.2 MTT assay

Mitochondrial enzymatic activity was estimated by MTT [3-(4,5-dimethylthiazol-2-yl)-2,5-diphenyltetrazolium bromide] assay (Sigma-Aldrich). A cell suspension of 10000 cells/well in 100 μL culture medium was seeded into 96-well plates. After each treatment with or without $1(\text{PF}_6)_3$ or $1(\text{NO}_3)_3$ salts, we changed the medium and then 10 μL of MTT (concentration equal to 1 mg/mL) were added to each well. After

incubation at 37°C for 4 hours, the formed purple formazan crystals were solubilized in 100 µL of lysis buffer (20% sodium dodecyl sulfate in 50% dimethylformamide) overnight at 37°C. Absorbance values were measured at 595 nm in a microplate reader (Synergy HT microplate reader (BioTek Instruments) and the results expressed as absorbance.

1.4 Antibacterial and antifungal activity

1.4.1 Microorganisms

The following strains were used for testing the antimicrobial activity of the salts: *Staphylococcus aureus* ATCC 6538, *Escherichia coli* ATCC 10536 and *Candida albicans* ATCC 10231. Bacteria were cultured in Tryptone Soya Broth (TSB, Oxoid, Basingstoke, UK) at 37 °C. The bacteria cultures were centrifuged at 3000 rpm for 20 min to separate cells from broth and then suspended in phosphate buffered saline (PBS, pH 7.3). The suspension was diluted to adjust the number of cells to 1×10^7 – 1×10^8 CFU/ml. *Candida albicans* was grown in Potato Dextrose Broth (PDB) (DIFCO, Detroit, MI, USA) for 24 h at 37 °C. The yeast culture was centrifuged at 3000 rpm for 20 min to separate cells from broth and then suspended in PBS (pH 7.3). The suspension was diluted to adjust the number of cells to 1×10^7 to 1×10^8 CFU/ml.

1.4.2 Evaluation of minimum inhibitory concentration (MIC) and minimum bactericidal-fungicidal concentration (MBC-MFC).

All the cage compounds ($1(\text{PF}_6)_3$ and $1(\text{NO}_3)_3$) were dissolved in dimethyl sulfoxide (DMSO) at different concentrations. These solutions were used in the determination of the antimicrobial activity against the reference strains. MICs and MBCs-MFCs were determined by twofold serial broth dilution method in Iso-Sensitest broth (ISB, Oxoid, Basingstoke, UK) according to Clinical and Laboratory Standards Institute (CLSI; formerly NCCLS) procedures[3]. The final concentration of DMSO in broth did not affect the microbial growth. The starting inoculum was 1.0×10^7 CFU/ml. Concentrations of cage compounds were tested in the range 1,95–255,00 µg/ml. Solvent blanks were included. The MIC was the lowest extract concentration inhibiting observable microbial growth after 24 h incubation at 37 °C. The MBC–MFC was the lowest concentration resulting in >99.9% reduction of the initial inoculum after 24 h incubation at 37 °C. All experiments were performed in triplicate[4]. Stock standard solutions of ampicillin and of amphotericin b were used as a positive control[5].

1.5 Anion transport studies

1.5.1 Procedure

1-Palmitoyl-2-oleoyl-sn-glycero-3-phosphocholine (POPC) was obtained from Avanti® Polar Lipids, Inc. Cholesterol was obtained from Sigma-Aldrich. Deacidified chloroform was obtained by passing chloroform through a column of basic alumina. An extrusion apparatus and 200 nm polycarbonate membranes were obtained from GC Technology Ltd. PD-10 Desalting Columns containing Sephadex G-25 Medium from GE Healthcare were used for size exclusion columns. All aqueous solutions were prepared using deionised water that had been passed through a Millipore filtration system.

POPC and cholesterol solutions in deacidified chloroform were combined in a 5 mL round bottom flask. Volumes of the aliquots were calculated from the concentrations of the lipid solution to obtain a POPC to cholesterol ratio of 7:3 (in general 4.20 μmol of POPC for 1.80 μmol of cholesterol). For experiments with preincorporated transporter, a solution of $1(\text{NO}_3)_3$ in methanol (100 μM , 24 μL , 2.4 nmol) was also added. The mole ratio of $1(\text{NO}_3)_3$ to lipid (POPC + cholesterol) was fixed at 1:2500 for all experiments. The solvents from the mixture were evaporated under a stream of N_2 and the resulting film was dried under high vacuum for 1 h. The residue was hydrated with 0.5 mL of an aqueous solution of 10,10'-dimethyl-9,9'-biacridinium nitrate (lucigenin, 0.8 mM) and NaNO_3 (225 mM), sonicated to suspend the lipids and stirred for 1 h to give heterogeneous vesicles. Multilamellar vesicles were disrupted by 10 freeze thaw cycles. The solution was loaded on the extrusion apparatus and the round bottom flask rinsed with 0.5 mL of aqueous NaNO_3 (225 mM). The solution was extruded 29 times through a polycarbonate membrane (200 nm pore size) to give a uniform distribution of LUVs with an average diameter of ~ 200 nm. The external lucigenin was removed by passing the solution through two prepacked size exclusion columns mounted in sequence. The vesicles were eluted with aqueous NaNO_3 (225 mM) and the elution was followed with a UV lamp (365 nm). The vesicles collected were further diluted with NaNO_3 solution (225 mM) to obtain the final vesicle solution (0.4 mM lipid). The vesicle solution (3.00 mL) was placed in a quartz cuvette with a stir bar and the fluorescence intensity (excitation at 430 nm, emission at 507 nm) was measured over time at 25 °C, using a Horiba FluoroMax+ fluorescence spectrometer.

For experiments with preincorporated $1(\text{NO}_3)_3$, aqueous NaCl (75 μL , 1.0 M in 225 mM aqueous NaNO_3) was added 30 seconds after the start of the experiment to give an external chloride concentration of 25 mM. The fluorescence intensity was measured for at least another 12 minutes after which 75 μL of Triton X-100 (5% volume in 225 mM aqueous NaNO_3) was added to break the vesicles.

For experiments with externally added $1(\text{NO}_3)_3$, the vesicle solution (3.00 mL) was placed in the fluorescence spectrometer and $1(\text{NO}_3)_3$ was added as a solution in methanol (4.5 μL) to give a mole ratio of lipid:transporter = 1:2500. Aqueous NaCl (75 μL , 1.0 M in 225 mM aqueous NaNO_3) was added 5 min after the addition of $1(\text{NO}_3)_3$ to give an external chloride concentration of 25 mM. The fluorescence intensity was

recorded for at least another 12 minutes after which 75 μL of Triton X-100 (5% volume in 225 mM aqueous NaNO_3) was added to break the vesicles.

2. Preparation of $1(\text{NO}_3)_3$

We synthesized the cage as described in a previous work by our group.[1] The cage as bromide salt (40.0 mg, 0.032 mmol) was dissolved in MeOH (5 mL) and treated with AgNO_3 (3 eqv, 0.0097 mmol, 16.4 mg). The mixture was stirred in the dark, at room temperature, for 1hr. The solid has been eliminated by filtering the solution on a pad of Celite. The collected solution was taken to dryness, under reduced pressure, and the raw product was obtained as a light grey powder. Purification was performed by dissolving the product in a small amount of hot MeOH, the insoluble residue was filtered off. This procedure was repeated twice. The solution was finally cooled to room temperature, and the final product was precipitated by addition of diethyl ether (white powder, 29.0 mg, yield: 76%).

$^1\text{H-NMR}$ (400 MHz, CD_3CN): δ 11.27 (s, 3H, H_α), 8.08 (s, 6H, H_1), 7.96-7.94 (m, 6H, H_5), 7.62-7.60 (m, 6H, H_6), 7.60-7.57 (d, 6H, H_4), 7.34 (t, 6H, H_3), 7.26 (d, 6H, H_2), 5.72 (s, 12H, H_b), 3.43 (s, 12H, H_a). $^{13}\text{C-NMR}$ (100 MHz, CD_3CN): δ 144.75 (C_α), 141.87 (q), 135.52 (q), 132.21 (q), 131.30 (C_1), 129.71 (C_4), 129.51 (C_3), 129.31 (C_2), 127.74 (C_6), 114.50 (C_5), 60.13 (C_a), 51.80 (C_b). HRMS-ESI (MeOH) m/z : $[\text{M}]^{3+}$ calculated for $\text{C}_{69}\text{H}_{63}\text{N}_8$, 334.5053, found 334.5042.

3. Characterization of 1(NO₃)₃

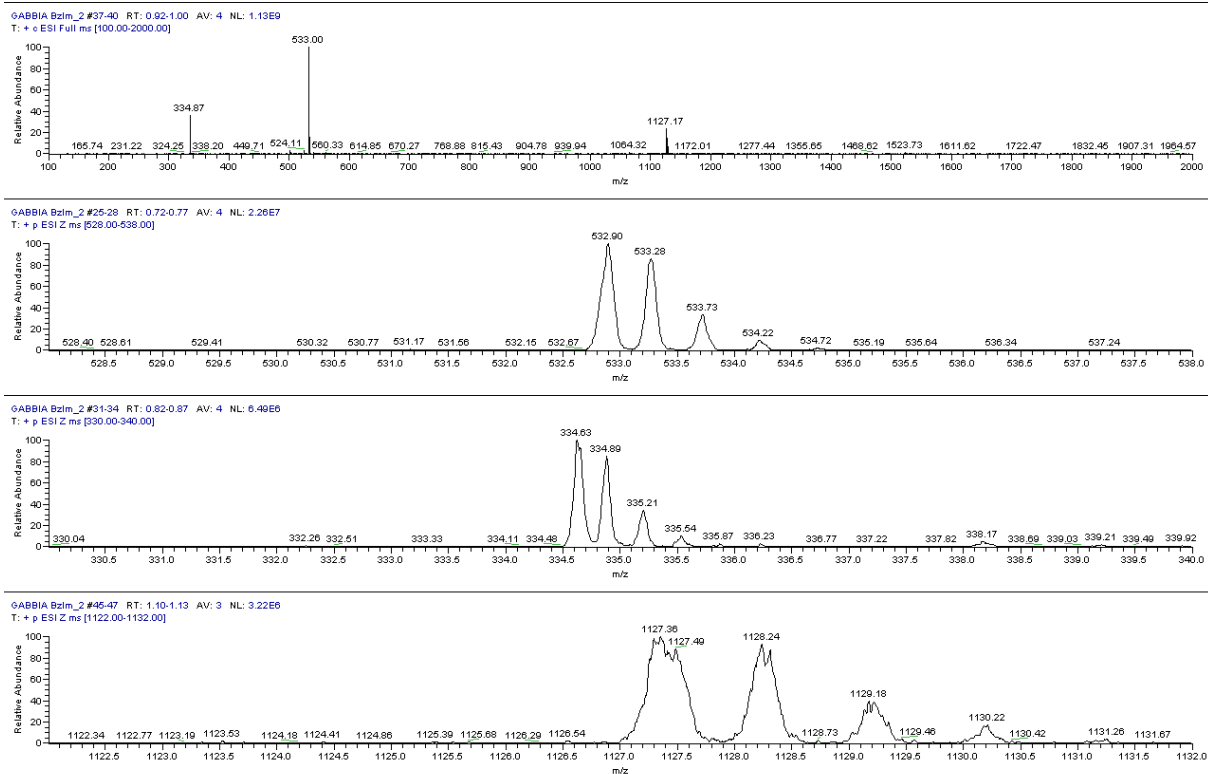


Figure S1: ESI-MS spectrum of 1(NO₃)₃ in MeOH. Peaks m/z: 334.87 [1]³⁺; 533.00 [1(NO₃)₂]²⁺; 1127.17 [1(NO₃)₂]⁺.

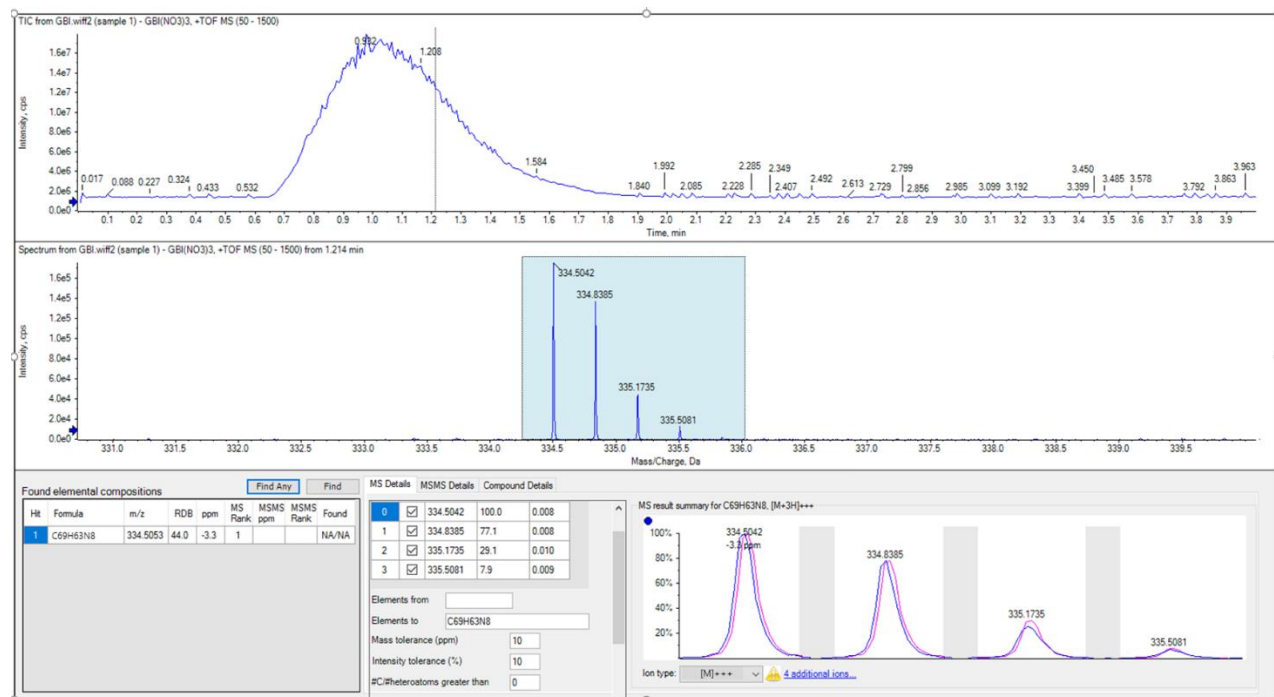


Figure S2: HRMS-ESI spectrum of 1(NO₃)₃ in MeOH

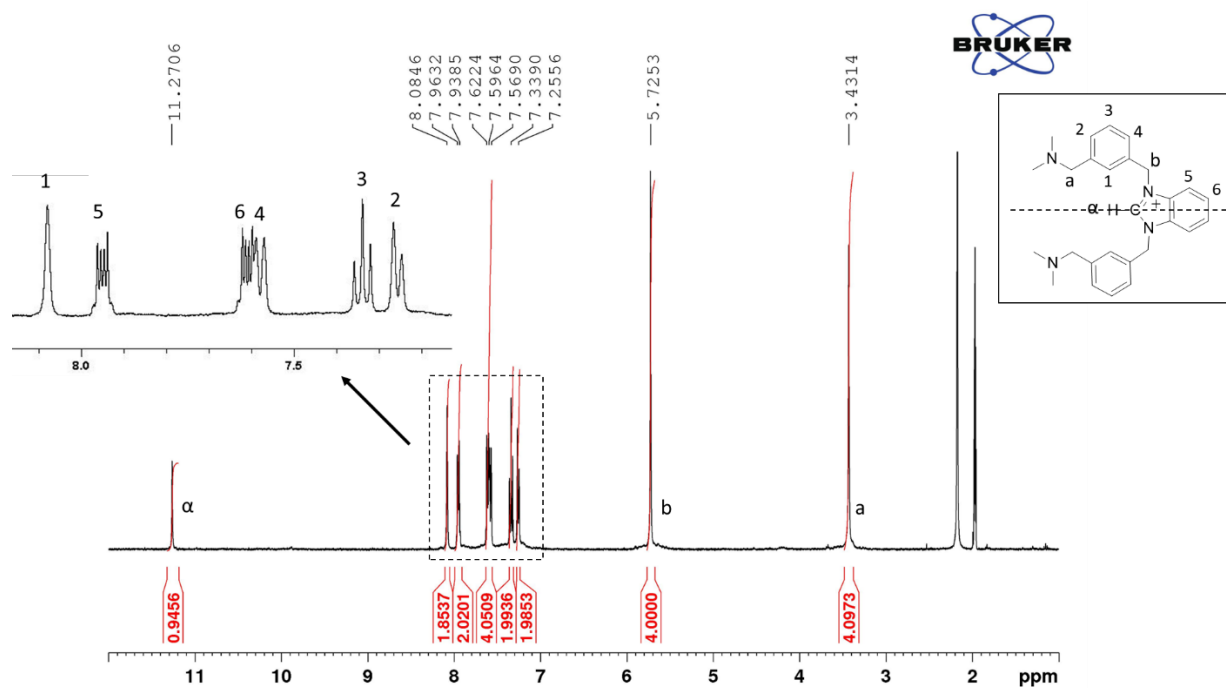


Figure S3: $^1\text{H-NMR}$ spectrum of $1(\text{NO}_3)_3$ in CD_3CN

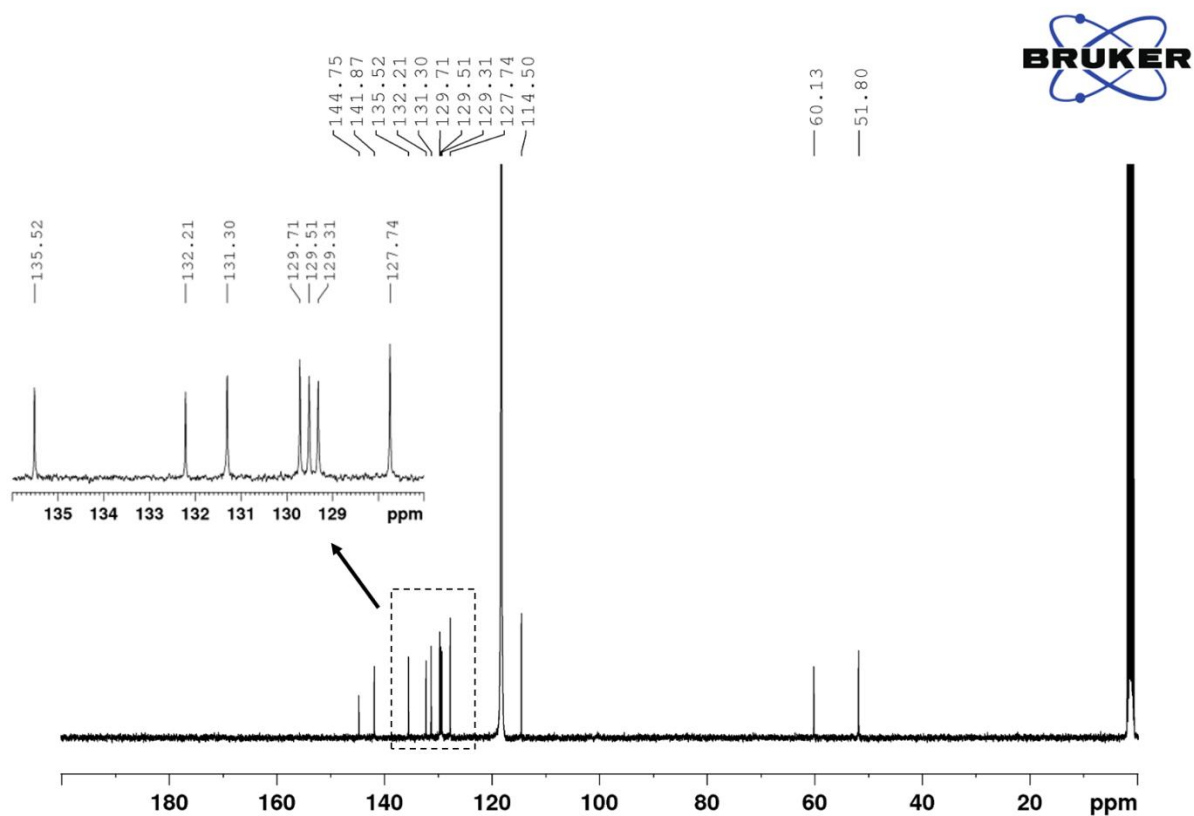


Figure S4: $^{13}\text{C-NMR}$ spectrum of $1(\text{NO}_3)_3$ in CD_3CN

4. Single crystals X-ray diffraction analysis

A crystal of $\mathbf{1}(\text{PF}_6)_3$ of with ca. $0.18 \times 0.10 \times 0.12$ mm as dimensions were selected and mounted on a MITIGEN holder in Paratone oil and very quickly placed on a liquid nitrogen stream cooled at 230 K to avoid the possible degradation upon dehydration. Diffraction data for $\mathbf{1}(\text{PF}_6)_3$ was collected using synchrotron at I19 beamline of the DIAMOND at $\lambda = 0.6889$ Å. The data were processed through CrysAlisPro[6] and xia2[7] software. The structure was solved with the SHELXS structure solution program, using the direct methods. The model was refined with version 2018/3 of SHELXTL against F^2 on all data by full-matrix least squares.[8] As reported in the main text, the structure of receptor **1** exhibits a remarkable flexibility.

The high flexibility observed in the crystal structure of $\mathbf{1}(\text{PF}_6)_3$, gave a high R agreement factor (see Table S1). To improve the quality of the refinement, we measured $\mathbf{1}(\text{PF}_6)_3$ at synchrotron and at low temperature, with the intention to reduce the severe thermal disorder observed for sample at room temperature, but, unfortunately, without successful results. Despite the high quality of the single crystals a severe thermal motion is constantly observed. In the light of these results, it is obvious that the modelled conformation of $\mathbf{1}(\text{PF}_6)_3$, is packed in the solid state through the cooperative but weak supramolecular interactions involving PF_6^- anions and ligand moieties. Statistical (and dynamic) disorder is seen very well and is certainly intrinsic to these systems. The most evident is the twist between the carbon atoms on the central nitrogen. The best model has been obtained when the positional disorder of the carbon atoms was defined. Unfortunately, around one of the two highly disordered rings there is also a lot of thermal disorder. But we are confident the crystal is reliable as the quality of data is very high with a resolution up to 2 θ of 60, measured with synchrotron light.

In the refinements of the crystal structure model, all non-hydrogen atoms were refined anisotropically. The use of some C-C bond lengths restraints has been reasonably imposed and related to the flexibility of cage's rings, that are dynamic components of the molecule. This was confirmed by very high thermal factor values observed. Because of a such disorder, alerts A and B in the checkcif are detected. The comments for the alerts are described in the CIFs using the validation response form (vrf).

The hydrogen atoms of the ligand were set in calculated positions and refined as riding atoms A summary of the crystallographic data and structure refinement for $\mathbf{1}(\text{PF}_6)_3$ (is given in Table S1).

CCDC reference number is CCDC 2193392

The final geometrical calculations on free voids and the graphical manipulations were carried out with PLATON[9] implemented in WinGX,[10] and CRYSTAL MAKER[11] programs, respectively.

Table S1. Summary of Crystallographic Data for 1(PF₆)₃.

Compound	1(PF ₆) ₃
Formula	C ₆₉ H ₆₃ N ₈ F ₁₈ P ₃
<i>M</i> (g mol ⁻¹)	1439.18
λ (Å)	0.6889
Crystal system	Orthorhombic
Space group	<i>Pna</i> 2 ₁
<i>a</i> (Å)	20.9197(2)
<i>b</i> (Å)	14.8105(2)
<i>c</i> (Å)	21.4828(2)
<i>V</i> (Å ³)	6656.04(13)
<i>Z</i>	4
ρ _{calc} (g cm ⁻³)	1.436
μ (mm ⁻¹)	0.135
<i>T</i> (K)	230
θ range for data collection (°)	1.619 to 30.836
Completeness to θ = 25.0	100%
Measured reflections	44202
Unique reflections (Rint)	20389 (0.0352)
Observed reflections [<i>I</i> > 2σ(<i>I</i>)]	9779
Goof	1.598
<i>R</i> ^a [<i>I</i> > 2σ(<i>I</i>)] (all data)	0.1627(0.2046)
<i>wR</i> ^b [<i>I</i> > 2σ(<i>I</i>)] (all data)	0.4143 (0.4433)
CCDC	2193392

^a $R = \sum(|F_o| - |F_c|) / \sum |F_o|$. ^b $wR = [\sum w(|F_o| - |F_c|)^2 / \sum w|F_o|^2]^{1/2}$.

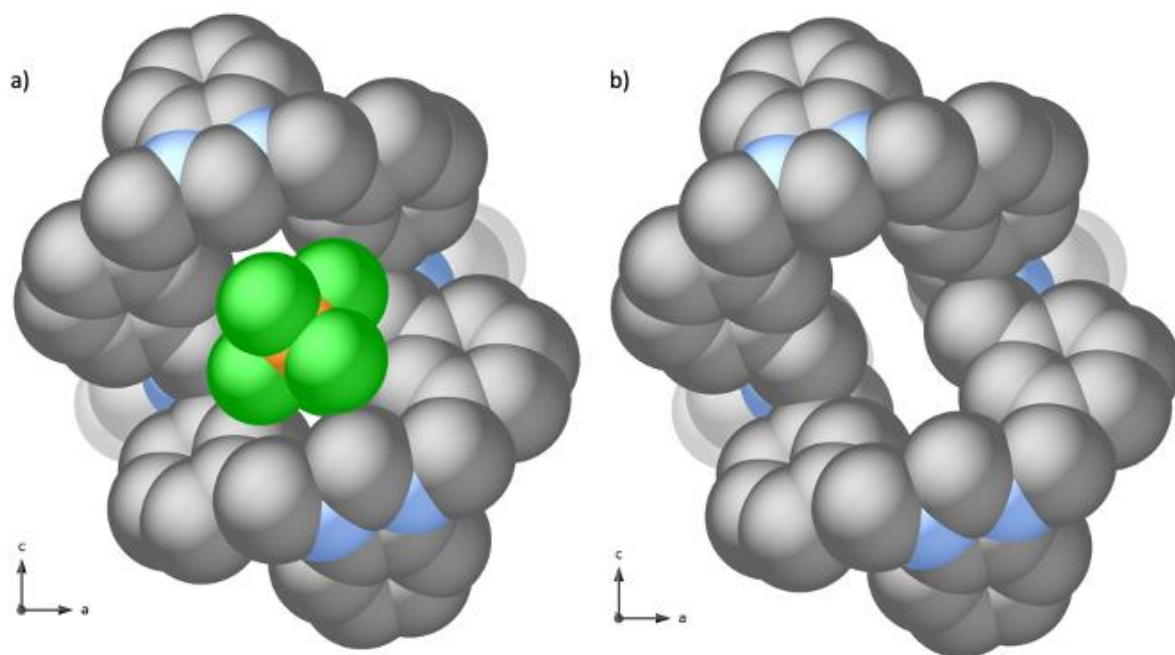


Figure S5: Perspective view of 1(PF₆)₃ crystal structure by space filling model (Van der Waals radii) exhibiting anions portion a) and the narrow window of the cage b). Hydrogen atoms are omitted for clarity. Color code: Carbon, grey; Nitrogen, sky blue; Phosphorus, orange; Fluorine, green.

5. ^1H -NMR investigations

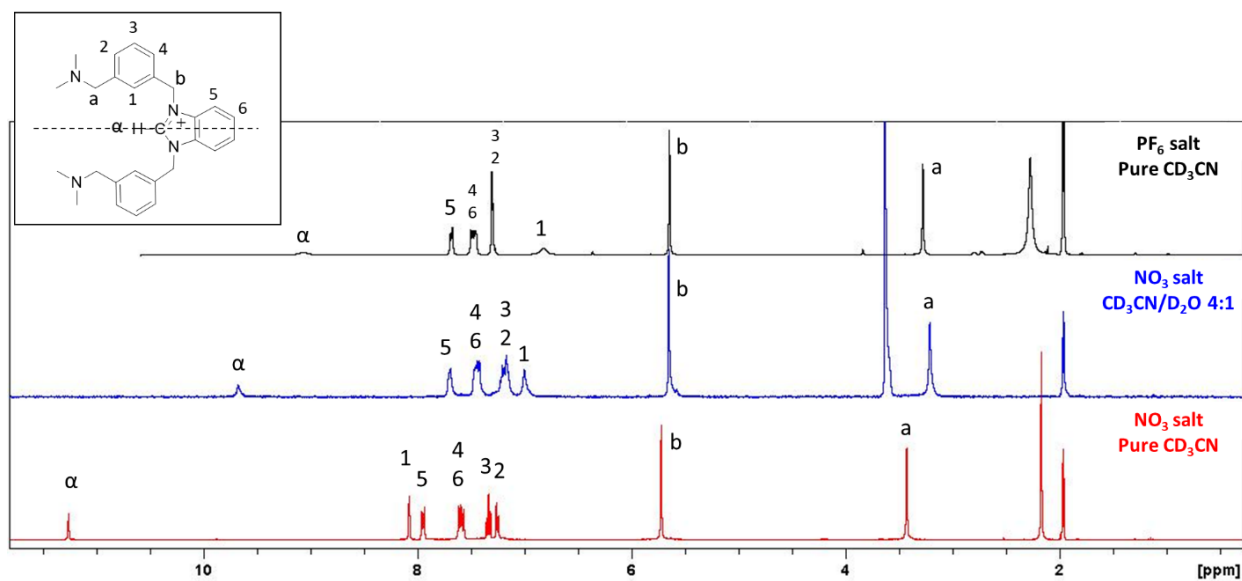


Figure S6: ^1H -NMR spectra of the two salts recorded in various deuterated solvents (25°C). The spectrum of $1(\text{PF}_6)_3$ was recorded in pure CD_3CN , while spectra of $1(\text{NO}_3)_3$ were recorded in both pure CD_3CN and $\text{CD}_3\text{CN}/\text{D}_2\text{O}$ 4:1 *v:v* mixture ($1(\text{PF}_6)_3$ is insoluble in these conditions).

5.1 ^1H -NMR titration of $1(\text{NO}_3)_3$ with chloride

The ^1H -NMR spectra recorded over the titration of $1(\text{NO}_3)_3$ with $[\text{TBA}]\text{Cl}$ are reported in Figure S6. The figure only shows the aromatic region of the NMR spectrum (between 6.5 and 9 ppm), because the chloride binding had a negligible effect on the aliphatic protons, Hb and Ha.

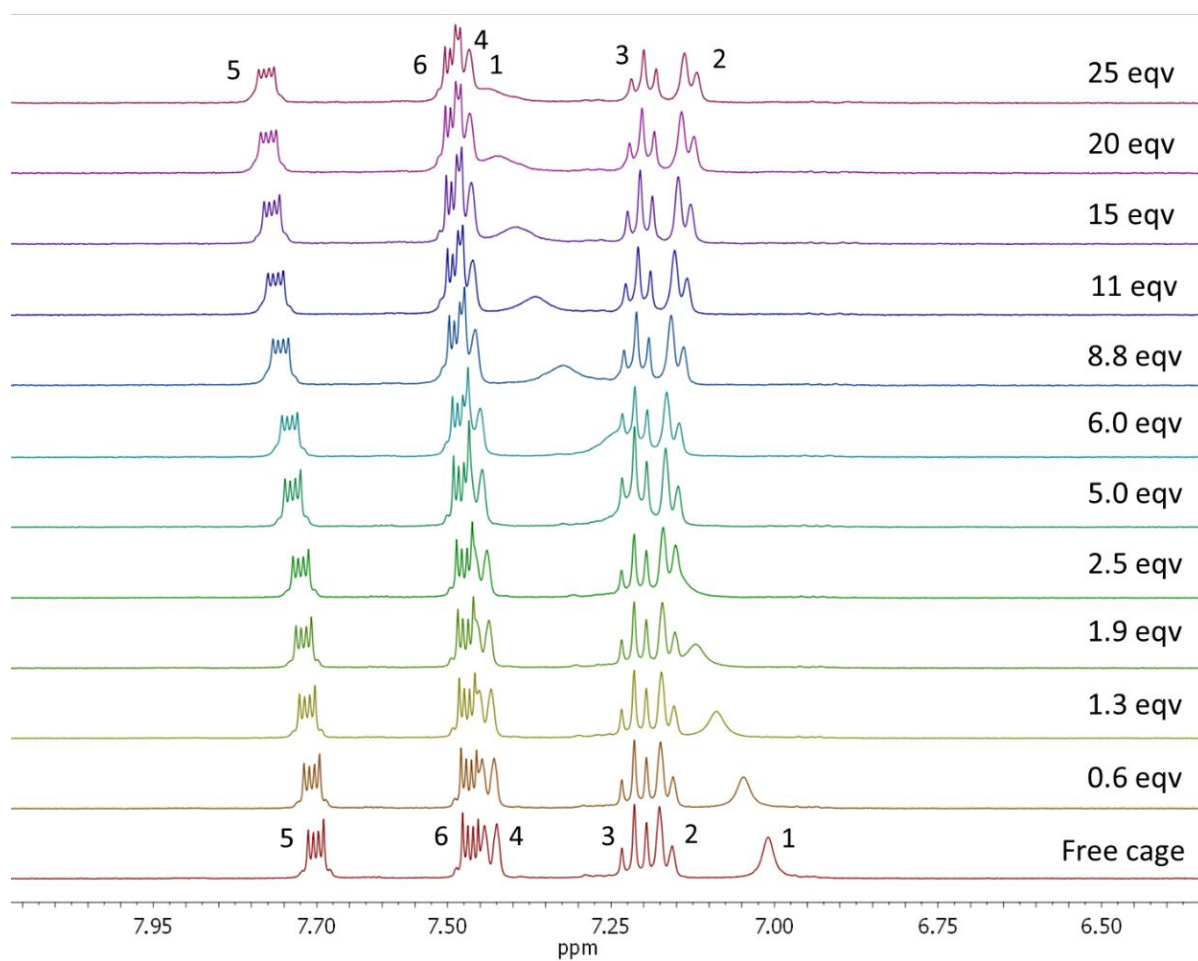


Figure S7: Family of ^1H -NMR spectra recorded over the course of titration of $1(\text{NO}_3)_3$ with $[\text{TBA}]\text{Cl}$ in $\text{CD}_3\text{CN}/\text{D}_2\text{O}$ 4:1 *v:v* mixture ($T = 25^\circ\text{C}$).

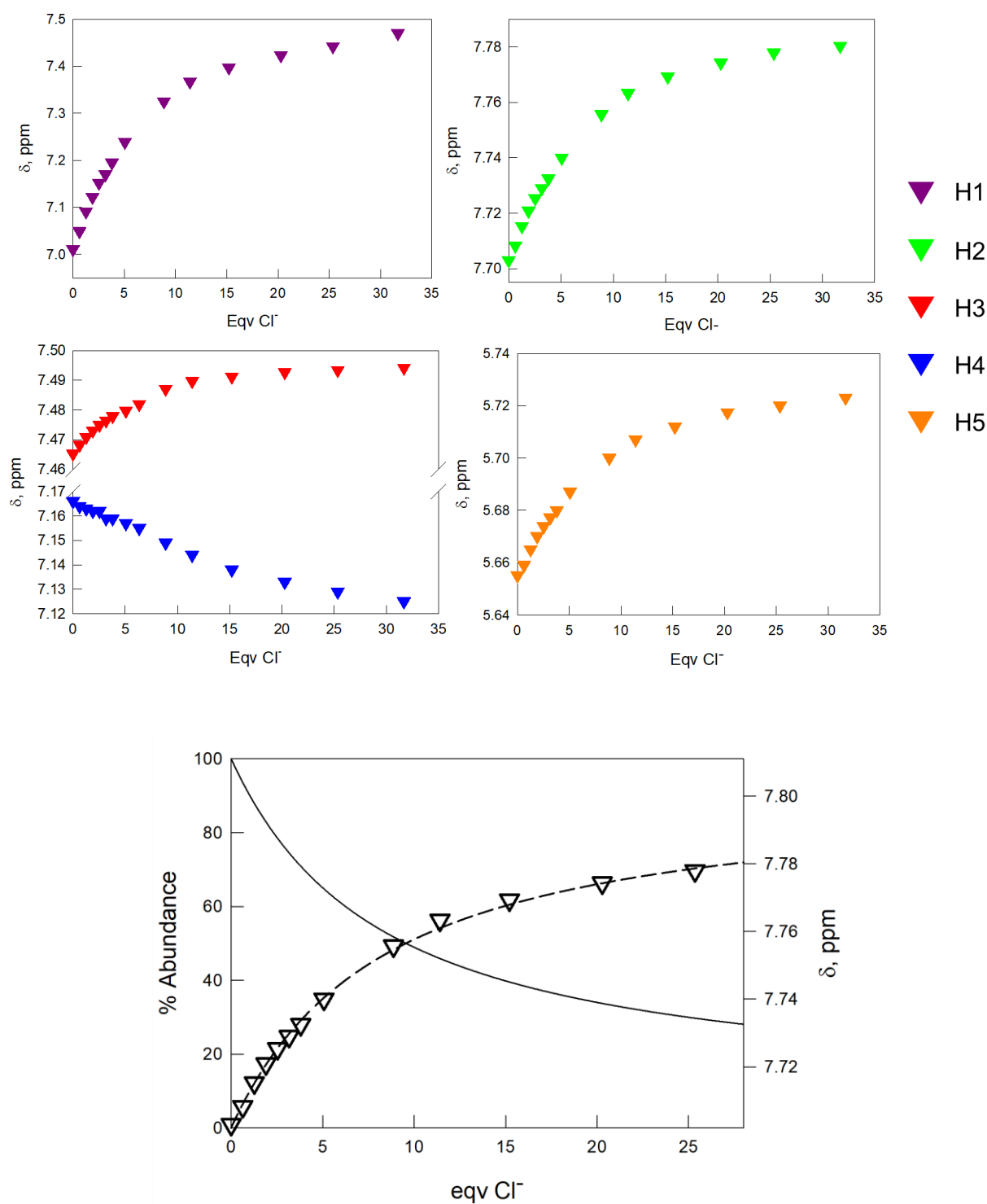


Figure S8: Titration profiles obtained by plotting the chemical shifts (δ ppm) of the most relevant protons of $1(\text{NO}_3)_3$ vs equivalents of the added $[\text{TBA}]\text{Cl}$. Bottom figure: titration profile for H2 with the superimposed distribution diagram species (1^{3+} : solid line; $1(\text{Cl})^{2+}$: dashed line) calculated for a $\text{Log}K_{11} = 1.53(2)$ ($T = 25^\circ\text{C}$).

5.2 NOE spectroscopy

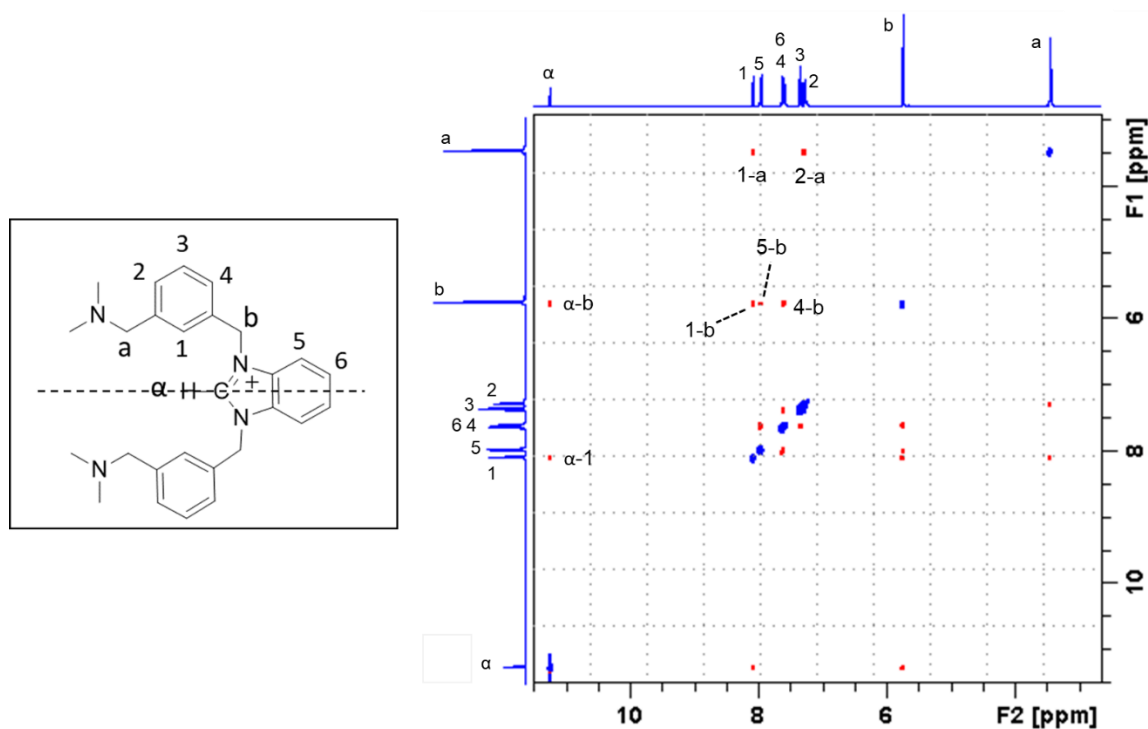


Figure S9: NOESY spectrum of **1**(PF₆)₃ in pure CD₃CN (T = 25°C).

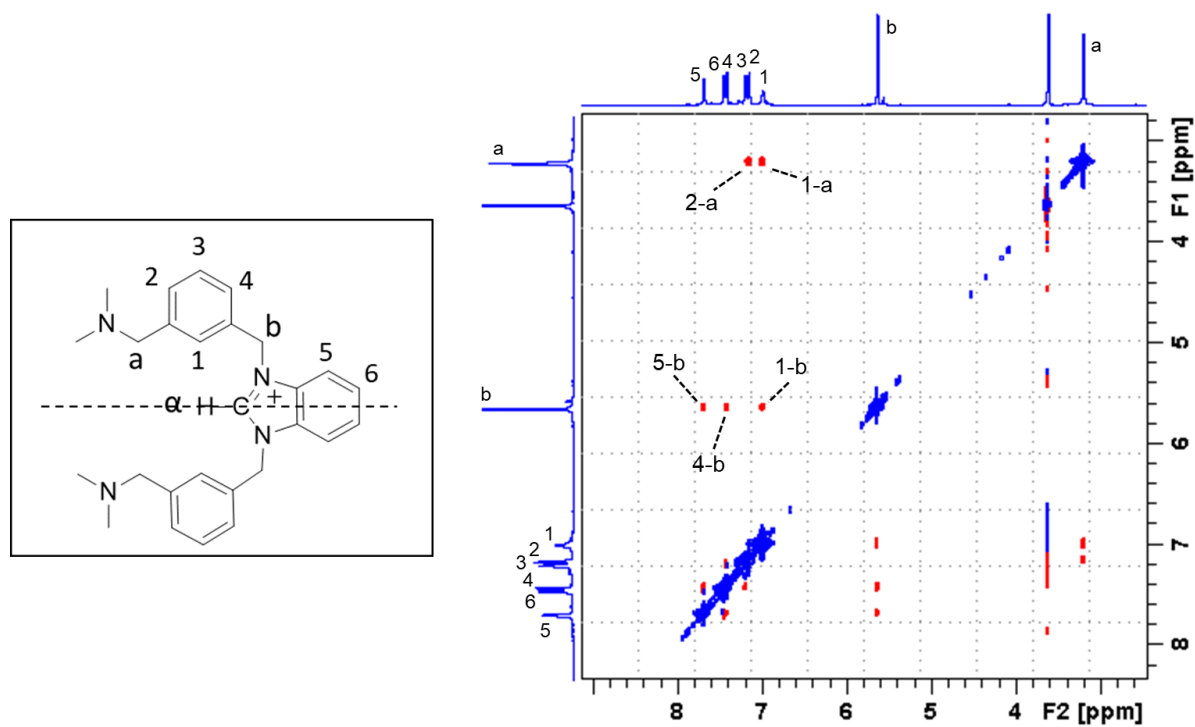


Figure S10: NOESY spectrum of **1**(NO₃)₃ in CD₃CN/D₂O 4:1(v:v) mixture (T = 25°C).

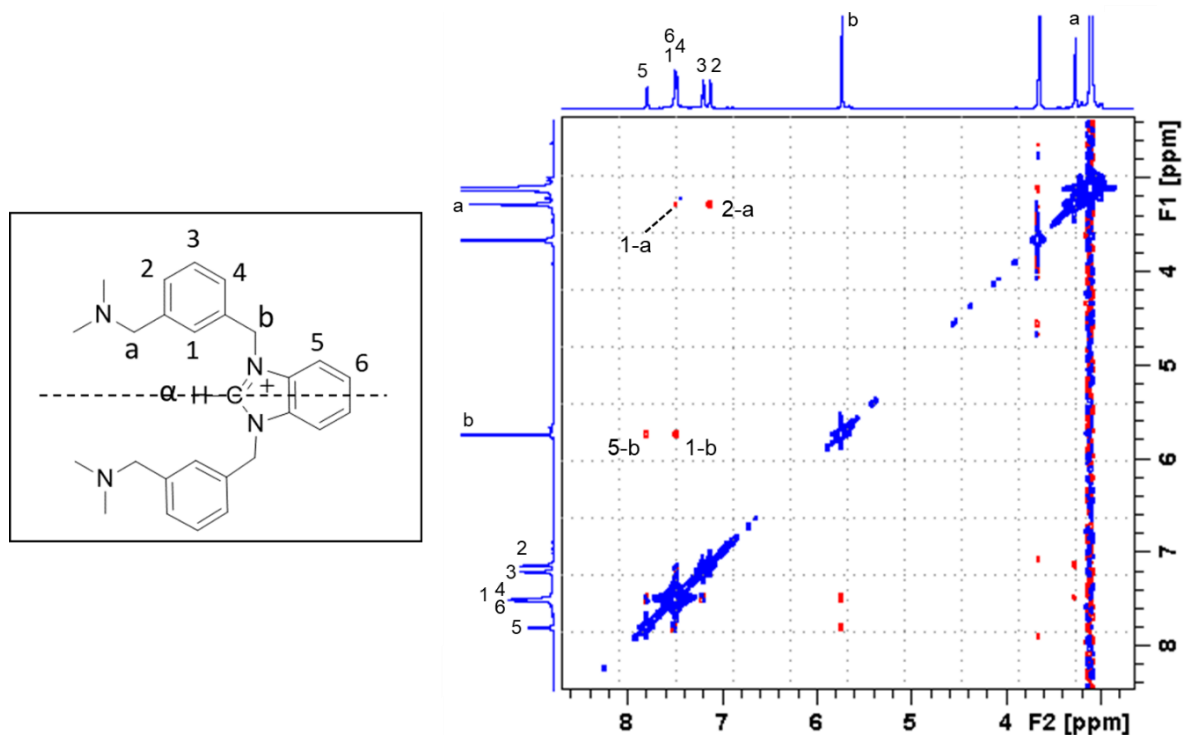


Figure S11: NOESY spectrum of the in situ prepared $[1(\text{Cl})]^{2+}$ complex in $\text{CD}_3\text{CN}/\text{D}_2\text{O}$ 4:1 mixture ($T = 25^\circ\text{C}$). For this experiment, an excess of $[\text{TBA}]\text{Cl}$ (30 eqv.) was added into the NMR tube containing a solution of $1(\text{NO}_3)_3$ in $\text{CD}_3\text{CN}/\text{D}_2\text{O}$ 4:1 (*v:v*) mixture.

6. Anion transport study on $1(\text{NO}_3)_3$

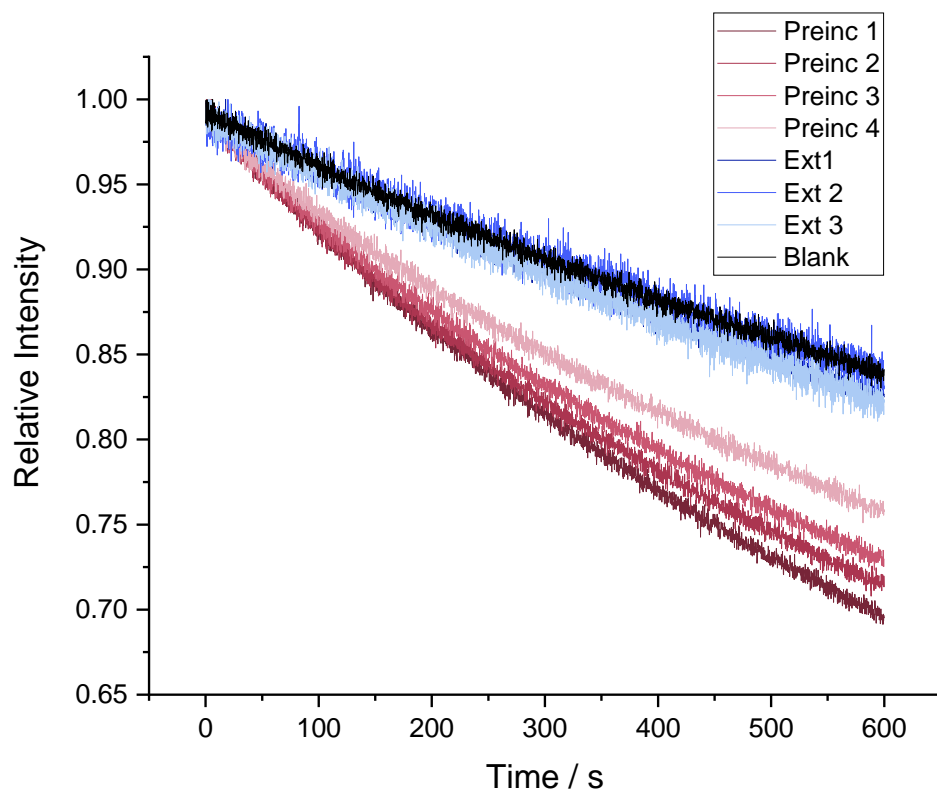


Figure S12: Chloride transport (25 mM) into 200 nm POPC:cholesterol (7:3) vesicle (0.4 mM lipid) in aqueous NaNO_3 (225 mM) by $1(\text{NO}_3)_3$. Preinc refers to experiments where the anionophore was preincorporated in the vesicle membranes, *i.e.* added to the lipids before vesicle formation (red traces, four experiments). Ext refers to experiments employing external addition, where $1(\text{NO}_3)_3$ was added to the preformed vesicles as a MeOH solution (4.5 μL) (blue traces, three experiments). In both cases the anionophore to lipid ratio was 1:2500. The blank (black trace) refers to the same experiment in the absence of anionophore.

References

- [1] Aletti, A.B.; Miljkovic, A.; Toma, L.; Bruno, R.; Armentano, D.; Gunnlaugsson, T.; Bergamaschi, G.; Amendola, V. Halide-Controlled Extending-Shrinking Motion of a Covalent Cage. *J. Org. Chem.* **2019**, *84*, 4221–4228.
- [2] Gans, P.; Sabatini, A.; Vacca, A. Investigation of equilibria in solution. Determination of equilibrium constants with the HYPERQUAD suite of programs. *Talanta* **1996**, *43*, 1739–1753.
- [3] Weinstein, M.P.; Patel, J.B.; Burnhman, C.-A.; Zimmer, B.L. M07-A Methods for Dilution Antimicrobial Susceptibility Tests for Bacteria that Grow Aerobically. *Clin. Lab. Stand. Inst.* **2012**, *32*, 1–67.
- [4] Barry, A.L. National Committee for Clinical Laboratory Standards. M26-A Methods for Determining Bactericidal Activity of Antimicrobial Agents; Approved Guideline This document provides procedures for determining the lethal activity of antimicrobial agents. *Clin. Lab. Stand. Inst.* **1999**, *19*, 1–14.
- [5] Brusotti, G.; Cesari, I.; Frassa, G.; Grisoli, P.; Dacarro, C.; Caccialanza, G. Antimicrobial properties of stem bark extracts from *Phyllanthus muellerianus* (Kuntze) *Excell. J. Ethnopharmacol.* **2011**, *135*, 797–800.
- [6] *CrysAlisPro*, 1.171.38.41; Rigaku Oxford Diffraction; Oxfordshire, England. 2015.
- [7] (a) Evans, P. Scaling and Assessment of Data Quality. *Acta Crystallogr. Sect. D Biol. Crystallogr.* **2006**, *62*, 72–82. (b) Evans, P. R.; Murshudov, G. N. How Good Are My Data and What Is the Resolution? *Acta Crystallogr. Sect. D Biol. Crystallogr.* **2013**, *69*, 1204–1214. (c) Winn, M. D.; Ballard, C. C.; Cowtan, K. D.; Dodson, E. J.; Emsley, P.; Evans, P. R.; Keegan, R. M.; Krissinel, E. B.; Leslie, A. G. W.; McCoy, A. et al. Overview of the CCP 4 Suite and Current Developments. *Acta Crystallogr. Sect. D Biol. Crystallogr.* **2011**, *67*, 235–242. (d) Winter, G. et al. An Expert System for Macromolecular Crystallography Data Reduction. *J. Appl. Crystallogr.* **2010**, *43*, 186–190.
- [8] (a) Sheldrick, G. M. Crystal Structure Refinement with SHELXL. *Acta Crystallogr. Sect. C Struct. Chem.* **2015**, *71*, 3–8. (b) Sheldrick, G. M. A Short History of SHELX. *Acta Crystallogr. A.* **2008**, *64*, 112–122.
- [9] Spek, A. L. Structure Validation in Chemical Crystallography. *Acta Crystallogr. D. Biol. Crystallogr.* **2009**, *65*, 148–155.
- [10] Farrugia, L. J. WinGX Suite for Small-Molecule Single-Crystal Crystallography. *J. Appl. Crystallogr.* **1999**, *32*, 837–838.
- [11] Palmer, D.C. *CrystalMaker*; CrystalMaker Software Ltd: Begbroke, Oxfordshire, England. 2014